



Multi-stimuli responsive bionic actuators constructed by linear liquid crystal polymers



Yu Pu, Xiaoyu Zhang, Xiaojun Liu, Xin Zhao, Ziyue Yang, Yanlei Yu*

Department of Materials Science and State Key Laboratory of Molecular Engineering of Polymers, Fudan University, Shanghai, 200433, China

ARTICLE INFO

Keywords:

Linear liquid crystal polymers
Ring-opening metathesis polymerization
Post-polymerization modification
Multi-stimuli responses
Bionic soft actuators

ABSTRACT

Liquid crystal polymers (LCPs) combine the entropic elasticity of polymers with the orderliness of LC mesogens, demonstrating outstanding performance across diverse applications, particularly in bionic actuators. In contrast to the organisms that enable multi-stimuli responsibility, most LCP actuators reported thus far exhibit responsiveness to only a single stimulus, hence the fabrication of multi-stimuli responsive LCPs is of pronounced significance. Here, a novel multi-stimuli responsive LCP is developed by integrating ring-opening metathesis polymerization (ROMP) and post-polymerization modification (PPM), which exhibits reversible responsiveness to humidity, light, and pH. By spray-coating the stretched polypropylene with LCP, the bilayer actuator loads exceed 20 times its weight upon exposure to light irradiation and moisture, showcasing exceptional output force. Furthermore, in response to the change in pH and humidity, the actuator exhibits behaviors akin to natural flowers, including blooming, closing, and color-changing. The strategy combining ROMP and PPM has proven to be a versatile strategy for the synthesis of multifunctional LCPs, offering transformative potential for the development of advanced bionic actuators and soft robotic systems.

1. Introduction

Natural organisms possess the remarkable self-adaptive ability that allows them to alter their properties in response to external stimuli and adapt to changing environments [1]. Inspired by these biomimetic principles, extensive efforts have been devoted to synthesizing, fabricating, and processing artificial materials to develop intelligent materials with stimulus-responsive capabilities [2–9]. Liquid crystal polymers (LCPs) combine the elasticity of polymer networks with the exceptional synergy of liquid crystal mesogens, which undergo reversible, programmable, and rapid changes in response to various stimuli such as thermal, electrical, magnetic, or optical fields [10,11]. Generally, most studies focus on the deformation or discoloration behavior of LCPs only in response to single stimulus [12–15]. In contrast, different environmental changes may occur simultaneously, therefore, the development of multi-stimuli responsive LCP holds significant promise for expanding the multifunctionality of devices, paving the way for innovative applications in biomimetic actuators and intelligent wearable technologies.

So far, several investigations focused on dual-stimuli responsive LCPs have been reported, most of which are characterized by the direct polymerization of monomers with functional groups [16–18]. Our

group first proposed a light- and humidity-responsive LCP by copolymerizing an azobenzene-containing monomer with a diacrylate cross-linker in a glass cell coated with alignment layers [19]. Due to the photoresponsive azobenzene and the humidity-responsive C=O and C-O-C, crosslinked LCP films bent toward the incidence direction of UV light and away from the moisture. Schenning et al. [20] prepared a dual-stimuli responsive crosslinked LCP by incorporating an azobenzene derivative Disperse Red 1 acrylate into a liquid crystal mixture consisting of hydrogen bonds. The LCP films with a splay orientation were prepared in liquid crystal cells, whose movements were controlled by a delicate interdependence between light and humidity. The above direct polymerization method suffers from limited group tolerance because many functional groups, especially polar groups, may lead to side reactions or hinder polymerization [21].

Post-polymerization modification (PPM), in which chemical modification is conducted after the polymerization, provides an alternative route to introduce function groups and miniatures the effects of side reactions [22,23]. Nevertheless, LCP precursors synthesized via (living) free radical polymerization typically have low molecular weight, leading to unsatisfactory mechanical properties and processability [24]. Therefore, reactive groups were mostly utilized for post-crosslinking reactions,

* Corresponding author.

E-mail address: ylyu@fudan.edu.cn (Y. Yu).

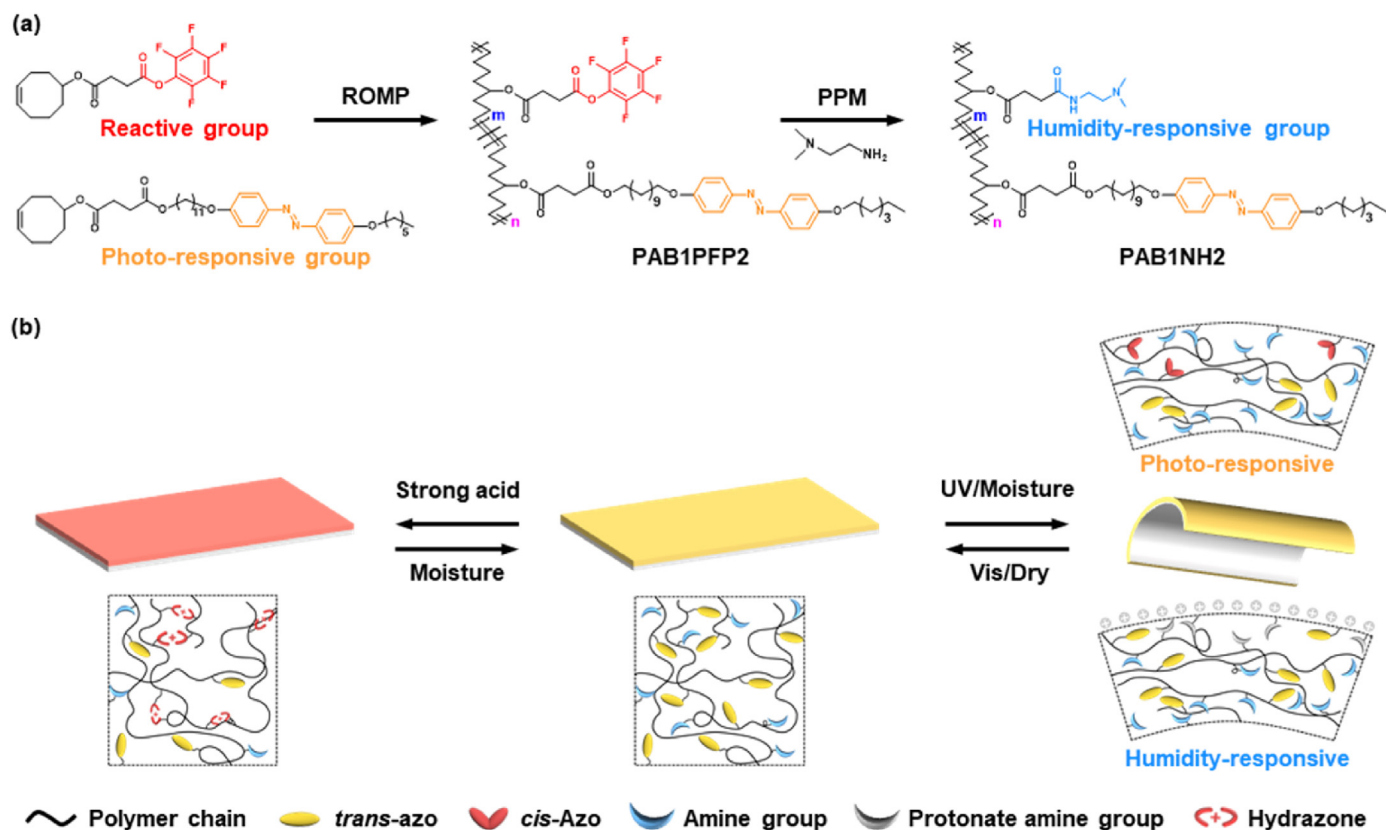


Fig. 1. Design of the multi-stimuli responsive actuator. (a) The synthetic route of the reactive LLC precursor (PAB1PFP2) and the multi-stimuli responsive LLC (PAB1NH2). (b) The mechanism for the multi-stimuli responsive actuator.

while the intrinsic advantages of PPM to multifunctionalize LCP precursors were not thoroughly exploited [25–27]. Our group previously reported a series of linear LCPs (LLCPs) synthesized through ring-opening metathesis polymerization (ROMP), which exhibited excellent mechanical properties endowed by high molecular weight [28]. Accordingly, we proposed a facile synthetic approach by combining ROMP with PPM to develop a light-/humidity-responsive LLC [29]. This approach involves ROMP to synthesize reactive polymer precursors with high molecular weight, followed by PPM to introduce functional groups through chemical modification, which provides a novel and effective strategy for preparing multifunctional LCP. Moreover, the LLC demonstrates compatibility with various processing methods such as solution casting and melt processing, showing the potential to construct multi-scale actuators from 1D to 3D. The facile strategy breaks the restriction of direct polymerization and has the potential to develop multi-stimuli responsive LCP and diverse bionic actuators.

In this work, we report a novel LLC that responds to light, humidity, and pH (Fig. 1). ROMP is responsible for the preparation of the highly reactive photoresponsive LLC precursor with the photo-responsive azobenzene mesogens. Subsequently, PPM is applied to introduce N,N-dimethylethylenediamine with humidity responsibility and miniaturize the effects of side reactions. Particularly, pH response characteristics are conferred by the synergistic effect of azobenzene and the N,N-dimethylethylenediamine group. Compared with crosslinked LCPs prepared by direct polymerization, LLCP with excellent processability is easily combined with stretched polypropylene membranes to fabricate bilayer film. The composite film demonstrates superior mechanical properties and deformation ability, which lifts the glass ball over 20 times its weight by humidity. Furthermore, the bionic flower actuator consisting of the bilayer film exhibits behaviors akin to natural flowers upon exposure to moisture and acid, including blooming, closing, and color-changing. The strategy of fabricating multi-stimuli

responsive LCPs facilitates the development of multifunctional bionic actuators and suggests the potential for the creation of novel intelligent materials.

2. Experimental procedures

2.1. Materials

4-Dimethylaminopyridine, Grubbs Catalyst 2nd Generation, 1-(3-dimethylaminopropyl)-3-ethylcarbodiimide hydrochloride, the reactive monomer pentafluorophenol, the humidity-responsive agent N,N-dimethylethylenediamine, hydrochloric acid and triethylamine were purchased from Adamas. Thionylchloride and anhydrous magnesium sulfate were purchased from Greagent. The commercial liquid crystal monomer 11-(4-((4-(hexyloxy)phenyl)diazanyl)phenoxy)undecan-1-ol was purchased from Hangzhou Yuhao Chemical Technology Co., Ltd. Butanedioic acid, mono-4-cycloocten-1-yl ester was purchased Chemsoon Co. Ltd. Anhydrous CH_2Cl_2 was distilled from CaH_2 before usage. Other conventional reagents and commonly used organic chemical solvents (such as methanol, ethanol, acetone, toluene, etc.) were purchased from Sinopharm Chemical Reagent Co., Ltd.

2.2. Synthesis of the reactive LLC precursor by ROMP (PAB1PFP2)

PAB1PFP2 was synthesized by copolymerizing the azobenzene-containing monomer and the pentafluorophenyl (PFP) ester-containing monomer by ROMP in a specific monomer ratio ($m:n = 2:1$). The polymerization was performed using standard Schlenk techniques under Argon atmosphere. Azobenzene-containing monomer (0.2 g, 0.3 mmol) and PFP ester-containing monomer (0.24 g, 0.6 mmol) were added into a Schlenk flask. Then, 0.3 μmol second-generation Grubbs catalyst with 5 mL anhydrous CH_2Cl_2 was added to the mixture. The mixture was stirred

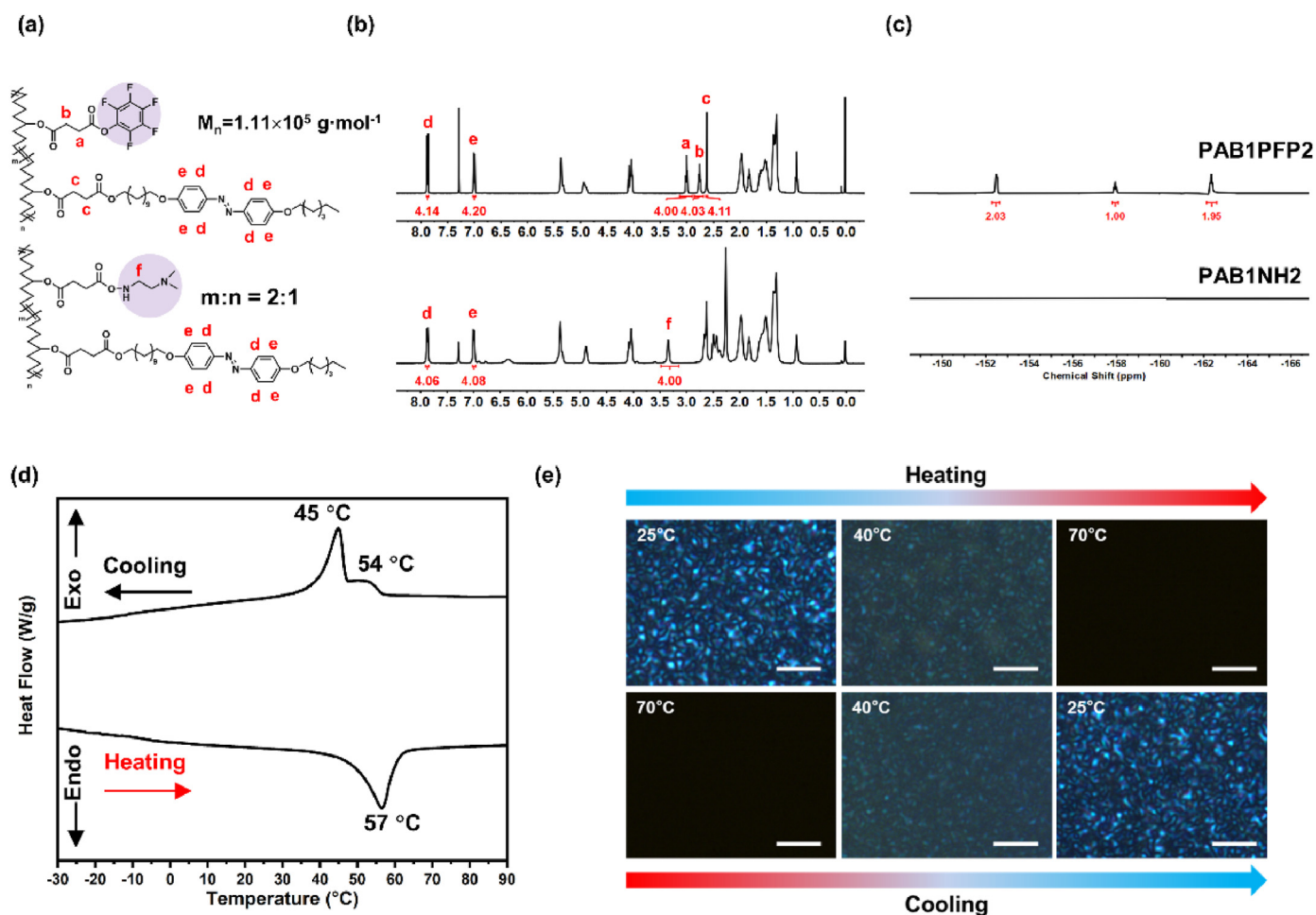


Fig. 2. Characterization of the PAB1PFP2 and PAB1NH2. (a) The chemical structures of LLCP precursor PAB1PFP2 and PAB1NH2 (b) The ^1H NMR spectra of PAB1PFP2 and PAB1NH2 in CDCl_3 (c) The ^{19}F NMR spectra of the PAB1PFP2 and PAB1NH2 before and after the PPM reaction. (d) DSC curves of PAB1NH2 during the second heating and cooling processes. (e) The POM images of mesogenic phase transitions of PAB1NH2 at varied temperatures from the second heating and cooling scans ($10\text{ }^\circ\text{C}/\text{min}$). Scale bar = $20\text{ }\mu\text{m}$.

at $45\text{ }^\circ\text{C}$ and held for 3 h under Argon atmosphere. The contents were then precipitated into cold methanol, filtered, and dried under vacuum to yield the PAB1PFP2 (0.40 g, 91 %).

2.3. Synthesis of the responsive LLCP by PPM (PAB1NH2)

PAB1PFP2 (0.22 g, 0.3 mmol of PFP ester group) and *N,N*-dimethylethylenediamine (0.08 g, 0.9 mmol) were dissolved in 5 mL of tetrahydrofuran (THF) in a 10 mL reaction vial and was placed in a preheated oil bath at $50\text{ }^\circ\text{C}$ with mechanical stirring for 24 h. The contents were added dropwise into methanol and then reprecipitated from THF in methanol twice. The product was dried under vacuum to obtain a yellow solid polymer (Yield, 82 %).

2.4. Preparation of the PAB1NH2/PP bilayer film

The PAB1NH2 (60 mg) was firstly dissolved in CH_2Cl_2 solution (2 mL) and the solution was coated by a spray bottle on the surface of the commercial CELGARD 2500 polypropylene (PP) film. The bilayer film was then dried in an oven at $40\text{ }^\circ\text{C}$ for 12 h, and the unsprayed part of the film was cut out.

2.5. Characterization of PAB1PFP2 and PAB1NH2

^1H NMR and ^{19}F NMR spectra of the synthesized monomer and LCP

were recorded on a Bruker AVANCE III HD NMR spectrometer using tetramethylsilane as the internal standard and CDCl_3 as the solvent (400 MHz). The molecular weight as well as the polydispersity index were measured by gel permeation chromatography (GPC, Waters, E2695) with THF as the eluent at a flow rate of 1 mL min^{-1} . Attenuated total reflection Fourier transform infrared (ATR-FTIR) spectra were recorded on a Bruker Vertex 70 spectrometer. The thermodynamic properties of the LLCs were determined by differential scanning calorimetry (DSC, TA, Q2000) at a heating and cooling rate of $10\text{ }^\circ\text{C}\cdot\text{min}^{-1}$. The textures of the LLCs were evaluated with a polarized optical microscope (POM, Leica, DM2500p) equipped with a hot stage (Linkam THMS600).

2.6. Mechanical and deformation properties of the PAB1NH2 film and microstructure of the PAB1NH2/PP bilayer film

The elastic modulus of the PAB1NH2 films was measured with a tensile machine (Instron, Series 5943) at a loading rate of 5 mm min^{-1} under ambient temperature and each test was repeated at least three times to allow a statistical analysis. Fatigue resistance was tested by 365 nm UV light generated by an Omron ZUV-H30MC light source with a ZUV-C30H controller and 530 nm visible light generated by a CCS HLV-24GR-3W for 20 cycles. The contact angle measurements before and after the "activation" process were investigated with the standard liquid quantity $3\text{ }\mu\text{L}$ (Dataphysics, OCA20). The surface and the cross-sectional morphologies of the PAB1NH2 and the PAB1NH2/PP bilayer film were

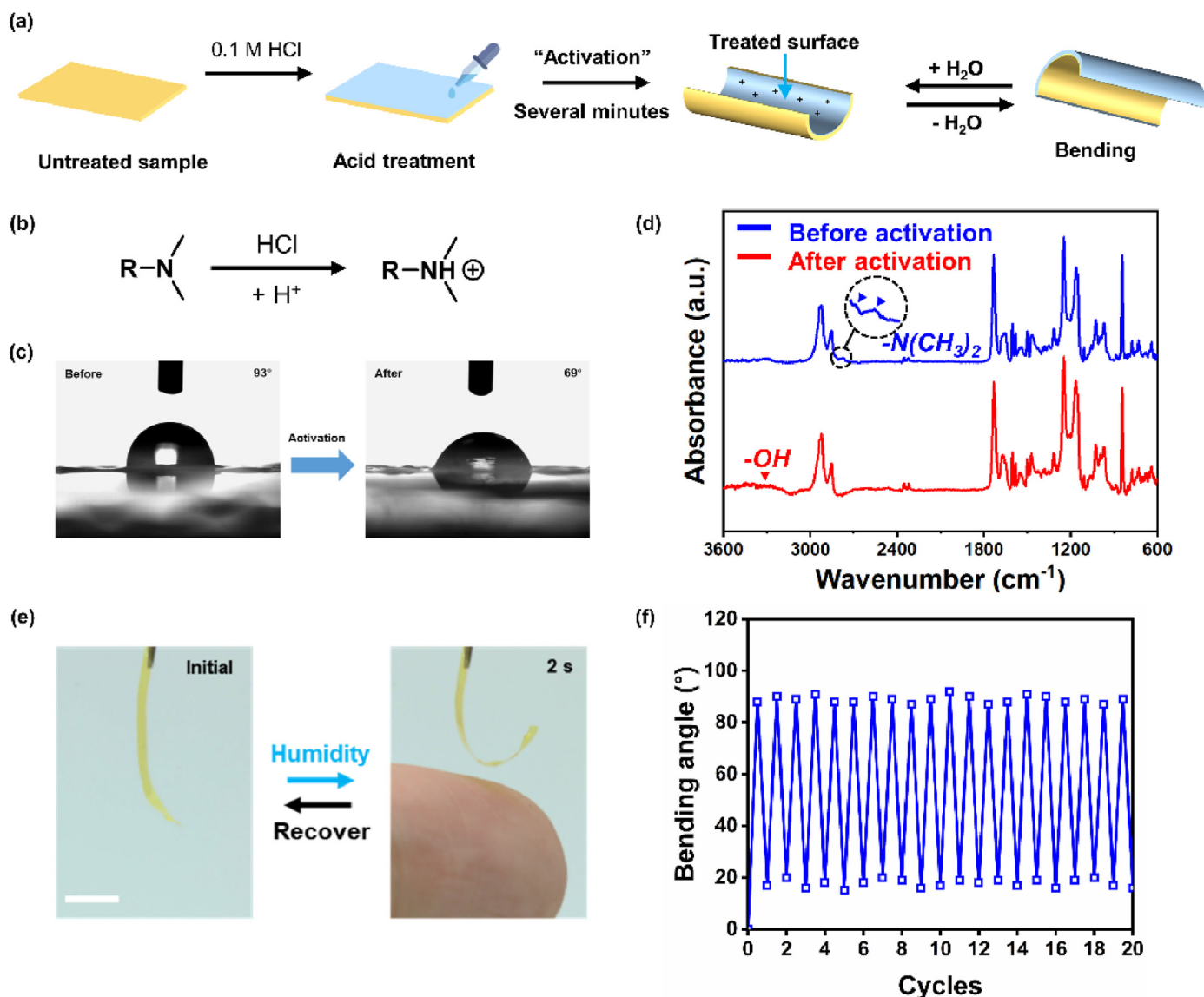


Fig. 3. Humidity-induced deformation of the PAB1NH2 film. (a) Schematic of the PAB1NH2 film activation by acidic solution (0.1 M HCl) and its humidity-responsive deformation. (b) Illustration showing the humidity-responsive mechanisms of the PAB1NH2 film. (c) The change of contact angle on the surface of the PAB1NH2 film before and after treatment with 0.1 M HCl. (d) ATR-FTIR spectra of the PAB1NH2 film before and after acidic treatment with 0.1 M HCl. (e) Photographs to show humidity-responsive behavior of acidic treated PAB1NH2 film on one side. Scale bar = 10 mm. (f) A plot showing the reversible deformation of the PAB1NH2 film upon cyclic exposure to humidity. The humidity-induced deformation repeats as many as 20 cycles without obvious fatigue.

observed by the scanning electron microscope (SEM, Zeiss, Ultra 55) with operating voltage at 3 kV.

3. Results and discussion

3.1. Chemical structure and the mesomorphic properties of PAB1NH2

PAB1NH2 was synthesized via a previously reported strategy that involved the combination of ROMP and PPM [29]. ROMP was utilized to synthesize a high-molecular-weight reactive LLCPP precursor (PAB1PPF2) with superior mechanical properties. The monomer selection was strategically based on their functional characteristics: an azobenzene-containing monomer was incorporated to confer photoresponsive properties, while another monomer with PFP ester was selected for its exceptional reactivity, rendering it highly suitable for the PPM modification. PPM has been demonstrated to be effective for the incorporation of a diverse range of functional groups, especially for those with polar characteristics. We investigated the multifunctionalization via

the aminolysis reaction of replacing the PFP ester in precursors to the humidity-sensitive *N,N*-dimethylethylenediamine group (Fig. 2a). The molecular weight of the resultant precursor was determined to be $1 \times 10^5 \text{ g mol}^{-1}$ via GPC analysis. The functionalization reaction of PAB1NH2 was confirmed through NMR spectra. The signals of the PFP esters disappear in the ¹⁹F NMR spectra (Fig. 2c), while new peaks, related to the hydrogen atom of *N,N*-dimethylethylenediamine, emerges in the ¹H NMR spectra after the aminolysis reaction (Fig. 2b). Additionally, the PFP ester allows for the flexible multifunctionalization of the reactive LLCPP precursors since the ester undergoes the nucleophilic substitution reaction to convert to various functional groups.

The functionalized PAB1NH2 retains its liquid crystalline properties even with the introduction of a non-liquid crystalline monomer, which was verified by DSC and POM with a hot stage. Fig. 2d demonstrates that the resultant PAB1NH2 exhibits relatively low glass transition temperature ($T_g \approx -10 \text{ }^\circ\text{C}$) and LC-to-isotropic phase transition temperature ($T_{iso} \approx 57 \text{ }^\circ\text{C}$), which are potentially due to the introduction of flexible dimethylamino groups. POM images of PAB1NH2 with corresponding

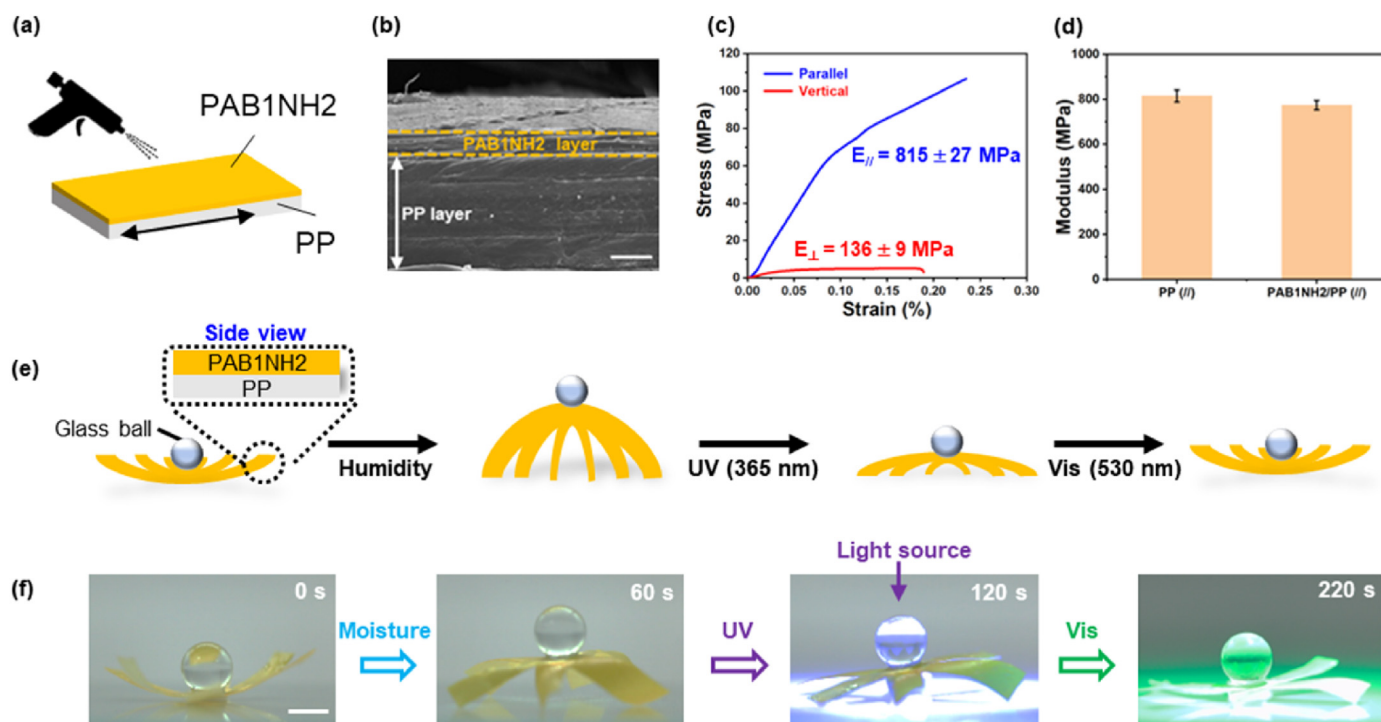


Fig. 4. The lifting micro robot with light and humidity response. (a) Schematic diagram of the spraying method for compositing PAB1NH2 and the commercial PP film. (b) SEM image of the PAB1NH2/PP bilayer film. Scale bar = 10 μm. (c) Stress-strain curves of the stretched PP film and (d) the elastic modulus of the PP and the PAB1NH2/PP films. (e) Schematic diagram of the functional execution of the lifting micro robot. (f) Photographs of the microrobot lifting/releasing an 850 mg glass ball under the stimulation of light and humidity. Scale bar = 10 mm.

phase transition temperatures exhibit obvious schlieren textures, revealing the presence of mesogenic phases (Fig. 2e), which also offers strong evidence of preservation after introducing the non-mesogenic moiety into the polymeric system. The above results suggest that the non-mesogenic moiety *N,N*-dimethylethylenediamine has less influence on the liquid crystallinity of the obtained PAB1NH2.

3.2. The humidity-responsive deformation of PAB1NH2

The humidity response of the PAB1NH2 film was attained by quaternizing dimethylamino groups via treatment with a low-pH solution, which allowed for the creation of cationic polymers. Similar to a previously reported method [30], only one side of the PAB1NH2 film was placed in contact with an acidic solution as the “activation” process (Fig. 3a, b). The increase in hydrophilicity on one surface of the PAB1NH2 film after activation induced asymmetric moisture sensitivity. The activated surface notably expanded when exposed to moisture, while the inactivated surface remained hydrophobic. Consequently, the activated PAB1NH2 film bent towards the inactivated surface due to the stress gradient throughout the direction of the film thickness. Charge generation on the activated LLCPP surface was confirmed through the contact angle measurement and the ATR-FTIR spectroscopy. The contact angle of the PAB1NH2 film significantly reduces from 93° to 69°, indicating an increase in the hydrophilicity of the surface treated with the acidic solution due to the generation of cations (Fig. 3c). It is also observed that the two peaks at 2750 and 2850 cm^{-1} corresponding to the stretching vibration of $-\text{N}(\text{CH}_3)_2$, disappeared after activation (Fig. 3d). This suggests that the dimethylamino groups have undergone protonation, resulting in the formation of $-\text{NH}^+(\text{CH}_3)_2$. The stronger electron-withdrawing effect of $-\text{NH}^+(\text{CH}_3)_2$ shifts these two peaks to a higher wavenumber, merging them with other peaks at 2940 cm^{-1} .

The humidity-induced deformation behavior is demonstrated in Fig. 3e. When a wet finger was brought near the acid-treated side of the PAB1NH2 strip, the strip immediately moved away from the finger-

approaching direction and the largest bending angle (θ) of about 90° was achieved within seconds. After removing the wet finger for 3–5 s, the strip automatically reverted to its original state (Supporting movie 1). Another significant phenomenon was that the strip displayed swift and stable deformation of 20 cycles when exposed to the changing ambient humidity, during which the bending angle of each cycle maintained a resemblance to the initial loop (Fig. 3f).

Supplementary data related to this article can be found online at <https://doi.org/10.1016/j.tramat.2025.100003>

3.3. Construction of the PAB1NH2/PP bilayer film

The multi-stimuli responsive bilayer film was prepared by spraying PAB1NH2 on a stretched PP film for the shape fixation of the soft actuator (Fig. 4a). The initial geometry of the actuator is controlled by the PP film, allowing arbitrary shapes to be achieved in a single sample. The PP film has multiple roles including both acting as the alignment layer to provide actuators with mechanical robustness and as a shape-programming polymer to create pre-designed initial geometries. Moreover, PAB1NH2 has good solubility due to the linear chemical structure and thus can be further sprayed to the PP film by the solution method. The SEM analysis demonstrates that the composite film is firmly bonded, composed of a 5-μm-thick PAB1NH2 layer and a 25-μm-thick PP layer with no apparent fracture or delamination at the intersection (Fig. 4b). The stress-strain curve in Fig. 4c illustrates that the PP film has an elastic modulus of 815 ± 27 MPa parallel to the stretching direction, whereas the elastic modulus is only 136 ± 9 MPa in the vertical direction, revealing its anisotropic mechanical property. According to the tensile results in Fig. 4d, the elastic modulus of the PAB1NH2 layer increases to 774 ± 21 MPa after combined with the PP film.

3.4. Actuation of the lifting micro robot

The PAB1NH2 layer of the composite film was further treated with

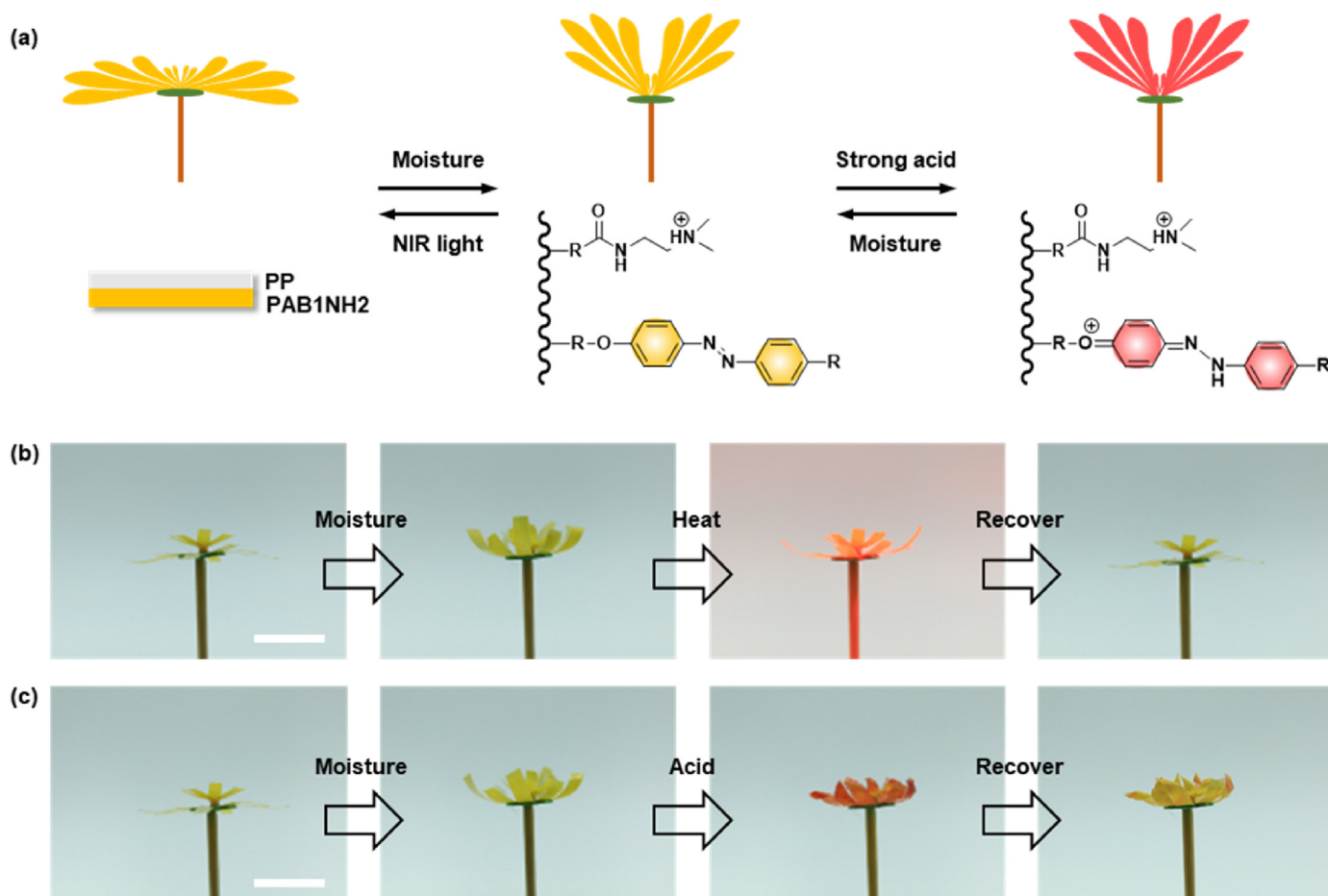


Fig. 5. The bionic flower actuator with humidity and pH response. (a) Schematic diagram and (b, c) Photographs of the blooming, closing, and color-changing behaviors of bionic flowers under the stimulation of humidity and strong acid. Scale bar = 10 mm.

0.1 M HCl solution to achieve the “activation” process, which exhibited the capacity for multifunctional responses to light, humidity, and pH. Subsequently, the self-supporting micro robot was prepared by the PAB1NH₂/PP bilayer film, capable of lifting the object with high output work (Fig. 4e, f). The 40 mg micro robot arched upwards to a height of 6 mm upon the humidity and elevated the 850 mg glass ball which is roughly 20 times heavier than the micro-robot itself. When exposed to UV light (100 mW/cm²), the photothermal effect induced an increase in the temperature of the bilayer film, facilitating moisture removal and thus leading to the flattening of the arched actuator. Concurrently, the hydrogen bonding in PAB1NH₂ enhances the stability of the *cis*-azobenzene, which indicates that a greater proportion of *cis* isomers are retained despite the rise in temperature resulting from the photothermal effect [31]. Subsequently, upon irradiation with green light, the azobenzene moieties underwent a transition from the *cis* to the *trans* form, resulting in the film eventually reverting to the initial state (Supporting movie 2). This micro robot possesses the capacity to reversibly lift objects by alternately humidity and light stimuli.

Supplementary data related to this article can be found online at <https://doi.org/10.1016/j.tramat.2025.100003>

3.5. Actuation of the bionic flower

Owing to the synergistic effect of the azobenzene and the N,N-dimethylethylenediamine, the PAB1NH₂/PP bilayer film displays acid-chromic and humidity-responsive performance. As a proof of concept, a flower-like actuator was created to mimic the blooming and closing behaviors of organisms (Fig. 5, Supporting movie 3). Upon exposure to

humidity stimulus, the film swiftly bent inward due to the surface expansion after moisture absorption, manifesting as the petal closure. Consequently, the bionic flower bloomed as the petals returned to their flattened state due to the loss of moisture upon the near-infrared light irradiation. In addition, the color of the petals converted conspicuously from the original yellow to magenta when exposed to the “acid rain” mimicked by the HCl solution (pH = 4), which recovered to yellow within 100 s upon exposure to distilled water vapor (pH = 7). This acid-chromic performance is attributed to the isomerization reaction of the azobenzene groups between their azo state and the hydrazone state. The transition from yellow to magenta color by decreasing pH is owing to the presence of the tertiary amine group [32]. The compound changes to the hydrazone state by proton transfer under acidic conditions caused by the protonation.

Supplementary data related to this article can be found online at <https://doi.org/10.1016/j.tramat.2025.100003>

4. Conclusion

In summary, we fabricated a multi-stimuli responsive LLCPC through ROMP and PPM. Utilizing the good processability of the LLCPC, we prepared the PAB1NH₂/PP bilayer films with robust mechanical properties. Further, bionic actuators with light-, humidity- and pH-response characteristics were assembled by tailoring. The lifting micro robot is capable of lifting a mass equivalent to 20 times its own weight, while the flower actuator is designed to emulate the blooming, closing, and color-changing processes akin to natural flowers. The successful construction of bio-inspired LLCPC actuators capable of responding to multiple stimuli,

derived from the combination of ROMP and PPM, demonstrates the potential for convenient implementation of a wide range of demanding functionalities. This strategy provides a versatile platform to create the multi-stimuli responsive bionic actuators and establishes a new toolbox for future bionic soft robotic devices.

CRedit authorship contribution statement

Yu Pu: Writing – review & editing, Writing – original draft, Visualization, Software, Investigation, Formal analysis. **Xiaoyu Zhang:** Investigation, Formal analysis, Data curation. **Xiaojun Liu:** Visualization, Validation, Resources, Data curation. **Xin Zhao:** Writing – original draft, Visualization, Investigation, Data curation. **Ziyue Yang:** Methodology, Investigation, Formal analysis. **Yanlei Yu:** Supervision, Resources, Project administration, Methodology, Funding acquisition.

Declaration of competing interest

The authors declare that they have no known competing financial interests or personal relationships that could have appeared to influence the work reported in this paper.

Acknowledgements

This work was supported financially from the National Natural Science Foundation of China (No. 52233001) and the Foundation of the Shanghai Municipal Education Commission (No. 2023ZKZD07, 24KXZNA05).

Appendix A. Supplementary data

Supplementary data to this article can be found online at <https://doi.org/10.1016/j.tramat.2025.100003>.

References

- B. Zou, Y. Chen, Y. Liu, R. Xie, Q. Du, T. Zhang, Y. Shen, B. Zheng, S. Li, J. Wu, W. Zhang, W. Huang, X. Huang, F. Huo, Repurposed leather with sensing capabilities for multifunctional electronic skin, *Adv. Sci.* 6 (2019) 1801283, <https://doi.org/10.1002/advs.201801283>.
- Y.X. Liu, C.M. Shao, Y. Wang, L.Y. Sun, Y.J. Zhao, Bio-inspired self-adhesive bright non-iridescent graphene pigments, *Matter* 1 (2019) 1581–1591, <https://doi.org/10.1016/j.matt.2019.08.018>.
- L. Chen, C. Lai, R. Marchewka, R.M. Berry, K.C. Tam, Use of CdS quantum dot-functionalized cellulose nanocrystal films for anti-counterfeiting applications, *Nanoscale* 8 (2016) 13288–13296, <https://doi.org/10.1039/C6NR03039D>.
- A. Belmonte, Y.Y. Ussembayev, T. Bus, I. Nys, K. Neyts, A.P.H.J. Schenning, Dual light and temperature responsive micrometer-sized structural color actuators, *Small* 16 (2020) 13288–13296, <https://doi.org/10.1002/sml.201905219>.
- M. Nie, C. Huang, X. Du, Recent advances in colour-tunable soft actuators, *Nanoscale* 13 (2021) 2780–2791, <https://doi.org/10.1039/D0NR07907C>.
- K. Li, Y. Shao, H. Yan, Z. Lu, K.J. Griffith, J. Yan, G. Wang, H. Fan, J. Lu, W. Huang, B. Bao, X. Liu, C. Hou, Q. Zhang, Y. Li, J. Yu, H. Wang, Lattice-contraction triggered synchronous electrochromic actuator, *Nat. Commun.* 9 (2018) 4798, <https://doi.org/10.1038/s41467-018-07241-7>.
- P. Zhang, G. Zhou, L.T. de Haan, A.P.H.J. Schenning, 4D chiral photonic actuators with switchable hyper-reflectivity, *Adv. Funct. Mater.* 31 (2021) 2007887, <https://doi.org/10.1002/adfm.202007887>.
- K. Meng, C. Yao, Q. Ma, Z. Xue, Y. Du, W. Liu, D. Yang, A reversibly responsive fluorochromic hydrogel based on lanthanide–mannose complex, *Adv. Sci.* 6 (2019) 1802112, <https://doi.org/10.1002/advs.201802112>.
- G. Lee, G.Y. Bae, J.H. Son, S. Lee, S.W. Kim, D. Kim, S.G. Lee, K. Cho, User-interactive therapeutic electronic skin based on stretchable thermochromic strain sensor, *Adv. Sci.* 7 (2020) 2001184, <https://doi.org/10.1002/advs.202001184>.
- S.W. Ula, N.A. Traugott, R.H. Volpe, R.R. Patel, K. Yu, C.M. Yakacki, Liquid crystal elastomers: an introduction and review of emerging technologies, *Liquid Crystals Reviews* 6 (2018) 78–107, <https://doi.org/10.1080/21680396.2018.1530155>.
- F. Brommel, D. Kramer, H. Finkelmann, Preparation of liquid crystalline elastomers, in: W. de Jeu (Ed.), *Liquid Crystal Elastomers: Materials and Applications*, Advances in Polymer Science, vol. 250, 2012, pp. 1–48, https://doi.org/10.1007/12_2012_168.
- L.T. Haan, J.M. Verjans, D.J. Broer, C.W. Bastiaansen, A.P. Schenning, Humidity-responsive liquid crystalline polymer actuators with an asymmetry in the molecular trigger that bend, fold, and curl, *J. Am. Chem. Soc.* 136 (2014) 10585–10588, <https://doi.org/10.1021/ja505475x>.
- K. Kamlesh, K. Christopher, B. David, M.A. Peletier, F. Heiner, S. Hecht, D.J. Broer, M.G. Debije, A.P.H.J. Schenning, A chaotic self-oscillating sunlight-driven polymer actuator, *Nat. Commun.* 7 (2016) 1–8, <https://doi.org/10.1038/ncomms11975>.
- J.K. Mu, C.Y. Hou, B.J. Zhu, H.Z. Wang, Y.G. Li, Q.H. Zhang, A multi-responsive water-driven actuator with instant and powerful performance for versatile applications, *Sci. Rep.* 5 (2014) 9503, <https://doi.org/10.1038/srep09503>.
- L.D. Zhang, H.R. Liang, J. Jacob, P. Naumov, Photogated humidity-driven motility, *Nat. Commun.* 6 (2015) 7429, <https://doi.org/10.1038/ncomms8429>.
- L.B. Braun, T. Hessberger, E. Pütz, C. Müller, F. Giesselmann, C.A. Serrac, R. Zentel, Actuating thermo- and photo-responsive tubes from liquid crystalline elastomers, *J. Mater. Chem. C* 6 (2018) 9093–9101, <https://doi.org/10.1039/C8TC02873>.
- J.M. Boothby, T.H. Ware, Dual-responsive, shape-switching bilayers enabled by liquid crystal elastomers, *Soft Matter* 13 (2017) 4349–4356, [https://doi.org/10.1016/S1359-6462\(97\)00072-9](https://doi.org/10.1016/S1359-6462(97)00072-9).
- B.T. Michal, B.M. McKenzie, S.E. Felder, S.J. Rowan, Metallo-, thermo-, and photoresponsive shape memory and actuating liquid crystalline elastomers, *Macromolecules* 48 (2015) 3239–3246, <https://doi.org/10.1021/acs.macromol.5b00646>.
- Y.Y. Liu, B. Xu, S.T. Sun, J. Wei, L.M. Wu, Y.L. Yu, Humidity- and photo-induced mechanical actuation of cross-linked liquid crystal polymers, *Adv. Mater.* 29 (2017) 1604792, <https://doi.org/10.1002/adma.201604792>.
- O.M. Wani, R. Verpaalen, H. Zeng, A. Priimagi, A.P.H.J. Schenning, An artificial nocturnal flower via humidity-gated photoactuation in liquid crystal networks, *Adv. Mater.* 31 (2019) 1805985, <https://doi.org/10.1002/adma.201805985>.
- A. Leitgeb, J. Wappel, C. Slugovc, The ROMP toolbox upgraded, *Polymer* 51 (2010) 2927e2946, <https://doi.org/10.1016/j.polymer.2010.05.002>.
- M.A. Gauthier, M.I. Gibson, H.A. Klok, Synthesis of functional polymers by post-polymerization modification, *Angew. Chem. Int. Ed.* 48 (2009) 48–58, <https://doi.org/10.1002/anie.200801951>.
- A. Das, P. Theato, Multifaceted synthetic route to functional polyacrylates by transesterification of poly(pentafluorophenyl acrylates), *Macromolecules* 48 (2015) 8695–8707, <https://doi.org/10.1021/acs.macromol.5b02293>.
- M. Eberhardt, R. Mruk, R. Zentel, P. Theato, Synthesis of pentafluorophenyl(meth)acrylate polymers: new precursor polymers for the synthesis of multifunctional materials, *Eur. Polym. J.* 41 (2005) 1569–1575, <https://doi.org/10.1016/j.eurpolymj.2005.01.025>.
- J.A. Lv, W. Wang, W. Wu, Y.L. Yu, A reactive azobenzene liquid-crystalline block copolymer as a promising material for practical application of light-driven soft actuators, *J. Mater. Chem. C* 3 (2015) 6621–6626, <https://doi.org/10.1039/C5TC00595G>.
- A. Das, P. Theato, Activated ester containing polymers: opportunities and challenges for the design of functional macromolecules, *Chem. Rev.* 116 (2016) 1434–1495, <https://doi.org/10.1021/acs.chemrev.5b02091>.
- Y. Chen, Q. Liu, P. Theato, J. Wei, Y.L. Yu, Activated ester containing polymers: opportunities and challenges for the design of functional macromolecules, *Adv. Intell. Syst.* 3 (2021) 2000254, <https://doi.org/10.1002/aisy.202000254>.
- J.A. Lv, Y.Y. Liu, J. Wei, E.Q. Chen, L. Qin, Y.L. Yu, Photocontrol of fluid slugs in liquid crystal polymer microactuators, *Nature* 537 (2016) 179–184, <https://doi.org/10.1038/nature19344>.
- X. Zhao, Y. Chen, B. Peng, J. Wei, Y.L. Yu, A facile strategy for the development of recyclable multifunctional liquid crystal polymers via post-polymerization modification and ring-opening metathesis polymerization, *Angew. Chem. Int. Ed.* 62 (2023) e202300699, <https://doi.org/10.1002/anie.202300699>.
- K. Kim, Y.H. Guo, J. Bae, S. Choi, H.Y. Song, S. Park, K. Hyun, S. Ahn, 4D printing of hygroscopic liquid crystal elastomer actuators, *Small* 17 (2021) 2100910, <https://doi.org/10.1002/sml.202100910>.
- Q.Y. Si, Y.Y. Feng, W.X. Yang, L.X. Fu, Q.H. Yan, L.Q. Dong, P. Long, W. Feng, Controllable and stable deformation of a self-healing photo-responsive supramolecular assembly for an optically actuated manipulator arm, *ACS Appl. Mater. Interfaces* 10 (2018) 29909–29917, <https://doi.org/10.1021/acsami.8b08025>.
- Development of acidochromic colloidal polymer nanoparticles containing azobenzene derivatives as eco-friendly time-dependent anticounterfeiting inks, *Eur. Polym. J.* 210 (2024) 112942, <https://doi.org/10.1016/j.eurpolymj.2024.112942>.